https://doi.org/10.5194/egusphere-2023-753
Preprint. Discussion started: 2 May 2023

Contribution of open ocean to the nutrient and phytoplankton inventory in a semi-enclosed coastal sea

Qian Leng[1], Xinyu Guo[2], Junying Zhu[3], Akihiko Morimoto[2]

[1]Graduate School of Science and Engineering, Ehime University, 2-5 Bunkyo-cho, Matsuyama, Ehime 790-8577, Japan
[2]Center for Marine Environmental Studies, Ehime University, 2-5 Bunkyo-cho, Matsuyama, Ehime 790-8577, Japan
[3]State Key Laboratory of Marine Resource Utilization in South China Sea, Hainan University, Haikou 570228, China

Correspondence to: Xinyu Guo (guoxinyu@sci.ehime-u.ac.jp)

Abstract. The semi-enclosed coastal seas serve as a transition zone between land and open ocean and their environments are therefore affected by both. The influences of land were noticed but that of the open ocean were usually neglected. The Seto Inland Sea (SIS), which is connected to the Pacific Ocean, is a typical representative of semi-enclosed seas. To quantitatively assess the inventory of nutrients originating from land and open ocean, and their supported phytoplankton in the SIS, we developed a three-dimensional coupled hydrodynamic-biogeochemical model and embedded a tracking technique in it. Model results showed that the open ocean contributes 73% and 60% to the annual inventory of dissolved inorganic nitrogen (DIN) and phytoplankton in the SIS, respectively. This proportion has apparent spatial variations: being highest near the boundary with the open ocean, decreasing from there towards the interior area of SIS, and being lowest in the nearshore areas. The open ocean imports 797 $mol\ s^{-1}$ of DIN to the SIS, 25% of which is consumed by biogeochemical processes, and 75% is delivered again to the open ocean. Such a large amount of oceanic nutrient input and its large contribution to the inventory of DIN and phytoplankton suggest the necessity to consider the impact of the open ocean variabilities in the management of land loading of nutrients for the semi-enclosed seas.

1 Introduction

The semi-enclosed coastal seas geographically refer to the seas surrounded by land and connected to the open ocean by one or more narrow entrances (Healy and Harada, 1991; Leppäkoski et al., 2009). These regions are highly productive due to their location at the transition zone between land and open ocean, which results in the receipt of nutrients from both terrestrial and oceanic sources (Bauer et al., 2013; Jickells, 1998). While it was previously believed that the narrow entrances limited the exchange between the semi-enclosed seas and the open ocean (Caddy, 2000; Statham, 2012), recent studies have highlighted the significant contribution of oceanic nutrients to the nutrient inventory in the semi-enclosed seas (Anderson et al., 2008; Mackas and Harrison, 1997; Townsend, 1998). Therefore, the role of oceanic nutrients cannot be disregarded in semi-enclosed seas. In fact, it has been known that the changes in terrestrial nutrients alone cannot fully explain ecological variations in these regions (Nakai et al., 2018).

https://doi.org/10.5194/egusphere-2023-753
Preprint. Discussion started: 2 May 2023

Unlike terrestrial nutrients, which are susceptible to anthropogenic activities, oceanic nutrients are typically regulated by climate change, which affects ocean currents and other environmental variables, including nutrient concentrations in the open ocean (Jickells, 1998; Vermaat et al., 2008). The transport process of oceanic nutrients into the coastal seas depends on the water exchange between the semi-enclosed seas and the open ocean, presenting a different seasonal variation from the terrestrial nutrients (Morimoto et al., 2022; Zhang et al., 2019). Because of its complex nature, the transport of oceanic nutrients into the semi-enclosed seas and their role in these seas are not easily known. One example is the Seto Inland Sea (SIS), where the presence of oceanic nutrients has been recognized for a long time (Hayami et al., 2004; Yanagi and Ishii, 2004). However, their transport flux into the SIS as well as their contribution to the primary production there have not been documented.

The impacts of an external source of nutrients are usually assessed by the amount of input into the coastal seas (Aoki et al., 2022), which actually reflects only its potential impact, not its real impact. One reason is that not all nutrients entering the coastal seas are available for phytoplankton growth (Zhang et al., 2019). Thus, the evaluation of the input amount of oceanic or terrestrial nutrients is only the first step in understanding their effects in semi-enclosed seas. Their real effects should be evaluated by their inventory of nutrients and biological particles (phytoplankton, zooplankton, and detritus) in the semi-enclosed seas, which is associated with the material flows in biogeochemical cycling and the material exchange at the boundary between semi-enclosed seas and open ocean.

In-situ observations can often be insufficient to differentiate materials originating from different sources of nutrients. To address this issue, researchers have proposed to introduce the tracking modules into the coupled hydrodynamic-biogeochemical models to trace the nutrients from different sources (Kawamiya, 2001; Ménesguen et al., 2006). Recently, this type of model has demonstrated their performance in quantifying the contribution of riverine and oceanic nitrogen to hypoxia formation in the Northern Gulf of Mexico, where the oceanic nitrogen supports 16±2% of summer sediment oxygen consumption (Große et al., 2019). Similar models have also been used to assess the contribution of different nutrient sources to primary production in the East China Sea, where the nutrients from the Kuroshio support up to 50% of primary production (Zhang et al., 2019).

This study focuses on the SIS, a semi-enclosed sea that is connected to the Pacific Ocean. Heavy eutrophication occurred in the SIS during the rapid economic growth of the 1960s -1970s due to urbanization and concentrations of industry and population around it. After that, Temporary Law for Environment Conservation in SIS and Special Law for Environment Conservation in SIS was made in 1973 and 1978, respectively. Based on the law, total amount controls of COD, nitrogen, and phosphorus have been conducted since then. As a result of a long time of effort, nutrient concentration has decreased in the SIS and concern about oligotrophication was raised for it (Yamamoto, 2003).

As the first step to understanding such long-term change in the nutrient concentrations in the SIS, we use a coupled hydrodynamic-biogeochemical model with a tracking technique to quantitatively evaluate the inventory of materials originating from the open ocean, river, and sediment. In addition, we emphasize the material flows involved in biogeochemical cycling and material exchange through the boundary with the open ocean. Through these analyses, we want to present an example to demonstrate the role of oceanic nutrients in semi-enclosed seas.

https://doi.org/10.5194/egusphere-2023-753
Preprint. Discussion started: 2 May 2023

2 Methods

2.1 Study area

The SIS is the largest semi-enclosed coastal sea in western Japan. It has a surface area of approximately 23,203 km2 and an average depth of 38 m (Fig. 1a). The sea is surrounded by three major islands, namely Honshu, Kyushu, and Shikoku, and is connected to the Pacific Ocean through two straits, the Bungo Channel and Kii Channel (Fig. 1b). During the summer, the cold and nutrient-rich Kuroshio subsurface water from the Pacific Ocean intrudes into the SIS through these two straits (Kobayashi and Fujiwara, 2009; Takashi et al., 2006; Guo et al., 2004). The SIS is surrounded by a highly industrialized area in Japan where more than 10 million people live. Consequently, the nutrients discharged from land are high (Yamamoto, 2003). Furthermore, the organic material in the sediment also releases nutrients (Tada et al., 2018; Yamamoto, 2003). Therefore, we consider three sources of nutrients for the SIS in this study.

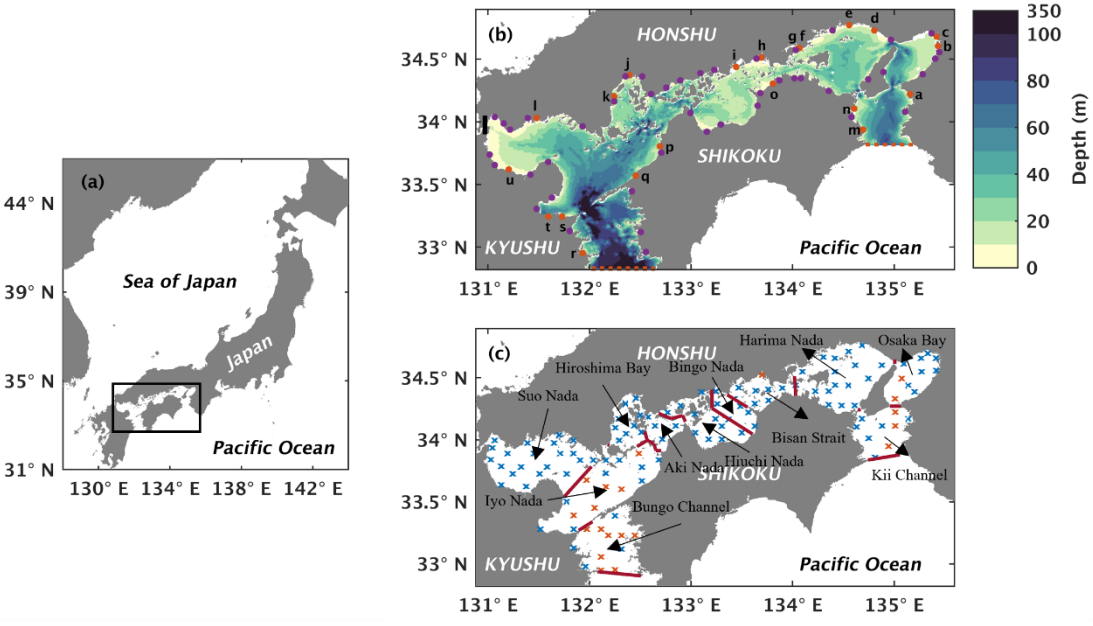

Figure 1. **(a)** Location of the Seto Inland Sea. **(b)** Bathymetry of the Seto Inland Sea. The solid orange circles with lowercase letters represent the locations of first-class rivers, and the solid purple circles represent the locations of second-class rivers. The names of 21 first-class rivers are shown in Table S2. The red dashed line in the west represents the open boundary between Bungo Channel and the open ocean, and the red dashed line in the east represents the open boundary between Kii Channel and the open ocean. The solid black line represents the location of Kanmon Strait. **(c)** Division of sub-regions and locations of in-situ observation stations. Red solid lines represent dividing lines of different sub-regions. Blue crosses represent in-situ observation stations with a depth of less than 50 m, and orange crosses represent in-situ observation stations with a depth greater than 50 m.

https://doi.org/10.5194/egusphere-2023-753
Preprint. Discussion started: 2 May 2023

2.2 Coupled hydrodynamic-biogeochemical model

A hydrodynamic model based on Princeton Ocean Model (Blumberg and Mellor, 1987) has been developed to simulate the climatological seasonal variation of water circulation in the SIS (Chang et al., 2009; Zhu et al., 2019). The model covered the entire SIS with a range from 32.8°N to 34.8°N and from 130.98°E to 135.5°E (Fig. 1), with two open boundaries south of Bungo Channel and Kii Channel connecting to the Pacific Ocean. The Kanmon Strait, which connects to the Japan Sea, was closed due to the poor water exchange there (Takeoka, 1984). 21 first-class rivers monitored by the Ministry of Land, Infrastructure and Transportation (MILT) and 45 second-class rivers monitored by the local government were specified along the coastline (Fig. 1b). The fluxes across the air-sea interface, including the momentum flux, mass flux, and heat flux, were from a daily dataset (Zhu et al., 2019). There were four tidal constituents, M_2, S_2, O_1, and K_1, in this model (Chang et al.,2009). The hydrodynamic model was used to obtain the water current field, temperature field, and diffusion coefficients for the biogeochemical model. For further information on the hydrodynamic model, including the initial and boundary conditions, please refer to Chang et al. (2009) and Zhu et al. (2019).

The biogeochemical model used in this study is a lower-trophic level model, which was employed to depict the annual nutrient and phytoplankton cycle in the coastal seas. It is a nitrogen-based model, and its structure is similar to the one proposed by Fasham et al. (1990). The model comprises five state variables, namely dissolved inorganic nitrogen (DIN), dissolved inorganic phosphate (DIP), phytoplankton (PHY), zooplankton (ZOO), and particulate organic matter (PON) (Fig. S1). The equations and parametric formulas governing the model were given in the supporting information. The parameter values were obtained from other marine ecosystem models (Fennel et al., 2006; Kishi et al., 2007; Xiu and Chai, 2014), and adjustments were slightly made for the SIS (Table S1).

The initial fields of DIN, DIP, and PHY were obtained from the Broad Comprehensive Water Quality Survey conducted by the Ministry of the Environment, Japan (https://water-pub.env.go.jp/water-pub/mizu-site/mizu/kouiki/dataMap.asp). Specifically, DIN, DIP, and PHY concentrations in January were averaged from 1981 to 2018 and used as the initial fields. As data for PON and ZOO were not available, the initial fields for these state variables were set to zero. This approach was considered reasonable as these variables are known to increase rapidly during the spin-up time (Fennel et al., 2006).

Regarding the air-sea interface, we used a daily dataset named third-generation Japanese Ocean Flux Data Sets with the Use of Remote-Sensing Observations (J-OFURO3) to provide the short-wave radiation flux that is used in the photosynthesis (Tomita et al., 2019). The daily dataset was averaged from 2002 to 2013 to obtain a daily climatological value.

To estimate the daily DIN load from rivers into the SIS, daily river discharge data and monthly nutrient concentration data from the Ministry of Land, Infrastructure and Transportation (MILT) were averaged over the period spanning from the 1990s to the 2010s. The spatial variation in DIN loads was observed among rivers, with high DIN loads being concentrated in the eastern part of the SIS, such as Osaka Bay and Harima Nada (Fig. S2). The DIN loads of all rivers showed a clear seasonal variation, with high loads in July and September and low loads in January, whose annual mean is 63.85 $mol\ s^{-1}$. Notably, the estimated DIN flux is smaller than the previously reported value, as previous studies also considered DIN from industrial

https://doi.org/10.5194/egusphere-2023-753
Preprint. Discussion started: 2 May 2023

sources and other land-based sources (Abo and Yamamoto, 2019; Tomita et al., 2016; Yamamoto, 2003). Furthermore, the model does not incorporate particle-based nitrogen input from rivers.

At the interface between the SIS and the open ocean, it is necessary to specify the nutrient concentrations at two open boundaries. Previous studies have shown that there is a good relationship between nutrient concentration and water temperature in the subsurface water of the Kuroshio Current (Morimoto et al., 2022; Takashi et al., 2006). In this study, we followed this idea and used the water temperature from the hydrodynamic model as a substitute for the observed water temperature to obtain nutrient concentrations at the open boundaries. To establish the relationship between water temperature and nutrient concentrations, we used observed monthly water temperature and nutrient concentrations in the Bungo Channel from 1991 to 2005, provided by the Fisheries Research Center, Ehime Prefectural Institute of Agriculture, Forestry and Fisheries, Japan (Fig. S3). As we lacked observed nutrient concentration data in the Kii Channel, we applied the Bungo Channel relationship to the Kii Channel, given that both channels are influenced by the subsurface water of the Kuroshio Current (Takashi et al., 2006). At the open boundaries in the Bungo Channel and Kii Channel, DIN concentration was high at the bottom throughout the year, with much higher concentrations in summer (Fig. S4). On the other hand, we lacked data for the concentrations of PHY, PON, and ZOO at the open boundaries, so we set their concentrations to zero. While we did not include the input of organic matter from the open ocean into the SIS, we allowed for the export of organic matter from the SIS by using the upwind scheme for tracer at the open boundaries.

At the water-sediment interface, the fluxes of PON ($mmol\ m^{-2}\ day^{-1}$) and DIN ($mg\ m^{-2}\ day^{-1}m$) were specified. To determine the downward PON flux to the sediment surface, we followed the method proposed by Wang (2002) and used Eq. (1):

$$Sediment\ PON\ flux = \begin{cases} C_b w_s \left(\frac{|\tau_b|}{\tau_c} - 1\right), & |\tau_b| < \tau_c \\ 0, & |\tau_b| \geq \tau_c, \end{cases} \quad (1)$$

where τ_c is the critical bottom stress. If the magnitude of bottom stress (τ_b) is larger than it, we assume no deposition occurs. We assigned τ_c a value of 0.14 $N\ m^{-2}$, by considering the sediment distribution in the SIS. τ_b ($N\ m^{-2}$) is calculated from the hydrodynamic model. C_b is the PON concentration ($mol\ m^{-3}$) in the bottom water. w_s is the sinking velocity of PON which was set at 1 $m\ day^{-1}$.

In addition to the downward PON flux, we also specify an upward DIN flux from the sediment using an empirical formula based on observation data (Tada et al., 2018). For the upward DIN flux from the sediment, we used Eq. (2):

$$Sediment\ DIN\ flux = \begin{cases} 1.802 * exp^{0.1277T} * (TN - 1.301), & TN > 1.301 \\ 0, & TN \leq 1.301, \end{cases}' \quad (2)$$

where T is the water temperature (℃) of the bottom water, and TN is the total nitrogen concentration ($mg\ g^{-1}$) at the sediment surface. T was calculated by the hydrodynamic model and applied to the biogeochemical model at each time step. The TN concentration at the sediment surface was the average value from the 1980s to 2010s obtained from the Seto Inland Sea Environmental Information Basic Survey (Ministry of the Environment, Japan; https://www.env.go.jp/water/heisa/heisa_net/setouchiNet/seto/g2/g2cat01/teishitsuodaku/index.html). The annual mean TN

https://doi.org/10.5194/egusphere-2023-753
Preprint. Discussion started: 2 May 2023

concentration was high in Suo Nada, Hiroshima Bay, Harima Nada, and Osaka Bay, but it was below the value of 1.301 $mg\ g^{-1}$ in Bungo Channel, Kii Channel, and Bisan Strait, where no DIN was released from the sediment (Fig. S5).

The hydrodynamic-biogeochemical model was initiated on the first day of January and stabilized from the third year onwards. Therefore, the simulation results of the third year were used to analyse the seasonal variations of DIN and PHY.

2.3 Tracking technique

In our study, we utilized the tracking technique proposed by Kawamiya (2001) and Ménesguen et al. (2006) in conjunction with the hydrodynamic-biogeochemical model. The nutrients in the SIS were considered to have three sources: oceanic, riverine, and benthic nutrients. To represent these sources, we introduced three additional sets of variables, namely DIN_{ocean}, PHY_{ocean}, PON_{ocean}, ZOO_{ocean}, DIN_{river}, PHY_{river}, PON_{river}, ZOO_{river}, and $DIN_{sediment}$, $PHY_{sediment}$, $PON_{sediment}$, $ZOO_{sediment}$, where the subscripts indicate the source. Each set of variables has its independent equations that are similar to the original equations for the sum of three sources of nutrients, i.e., DIN , PHY , PON , ZOO . The complete governing equations for the tracked variables are provided in the Supplement Materials. Regarding the hydrodynamic processes, all tracked variables have the same advection and diffusion terms. However, for the biogeochemical processes, the tracked variables have a different form. Here, we describe how the biogeochemical terms of tracked variables were treated in our study. Regarding the biogeochemical processes in the model, we calculated the flux that converts one variable to another one (Fig. S1), denoted as $Flux_{A\to B}$, where A was the variable being converted, and B was the target variable. The contribution of each nutrient source to the biogeochemical process depends on its proportion in the total concentration of the variable being converted, as described by Eq. (3), (4), and (5):

$$Flux_{A\to B}^{ocean} = Flux_{A\to B}\frac{[A_{ocean}]}{[A]}, \quad (3)$$

$$Flux_{A\to B}^{river} = Flux_{A\to B}\frac{[A_{river}]}{[A]}, \quad (4)$$

$$Flux_{A\to B}^{sediment} = Flux_{A\to B}\frac{[A_{sediment}]}{[A]}, \quad (5)$$

where the bracket denotes the concentration and $[A] = [A_{ocean}] + [A_{river}] + [A_{sediment}]$. $[A]$ can be any of 4 variables (DIN , PHY , PON , ZOO) used in the model.

We initiated the tracking technique from the first day of the fourth year of the hydrodynamic-biogeochemical model, with a value of zero for the initial fields of all the variables originating from the three sources of nutrients. DIN_{ocean} had the same values as those used at the open boundaries of the hydrodynamic-biogeochemical model but was specified to zero at the land-sea interface and the water-sediment interface. DIN_{river} at the land-sea interface was identical to those used in the hydrodynamic-biogeochemical model, but it was set to zero at the open boundaries and water-sediment interface. $DIN_{sediment}$ was set to have the same flux at the sediment-water interface as that in the hydrodynamic-biogeochemical model, but it was set to have zero flux at the open boundaries and land-sea interface. The other model configurations of the tracking technique

https://doi.org/10.5194/egusphere-2023-753
Preprint. Discussion started: 2 May 2023

were the same as those of the hydrodynamic-biogeochemical model. After a spin-up of three years, the annual cycle of each source of nutrients and related particles became stationary.

2.4 Validation data

We obtained the observation data to validate the seasonal and spatial distribution of DIN and PHY from the Broad Comprehensive Water Quality Survey, Ministry of the Environment, Japan (https://water-pub.env.go.jp/water-pub/mizu-site/mizu/kouiki/dataMap.asp). The original data were collected at 121 stations distributed throughout the SIS during January (winter), May (spring), July (summer), and October (autumn) (Fig. 1c). At each station, the data were from two layers, the surface layer, which was 1 m below the sea surface, and the bottom layer, which was 1 m above the sea bottom for stations shallower than 50 m and 50 m depth for stations deeper than 50 m. We used the averaged field from 1981 to 2021, i.e., a climatological field, to validate our model results.

3 Results

3.1 Seasonal and spatial variations of DIN and PHY

At the surface layer, the observed DIN concentration was low in May (Fig. 2b) and July (Fig. 2c), with a value around 0.5 $mmol\ m^{-3}$, as most of DIN was consumed by PHY for its growth. At the bottom layer, the observed DIN concentration remained relatively stable throughout the year, with a value over 2 $mmol\ m^{-3}$ in most areas, except for May, when it appeared slightly lower at a value around 1.5 $mmol\ m^{-3}$ (Fig. 2f). The observed DIN concentration was well mixed vertically in January (Fig. 2a, 2e) because the stratification disappeared from late autumn to winter (Chang et al., 2009; Takeoka, 1985). In July, the high DIN concentration at the bottom layers of the Bungo Channel and Kii Channel (Fig. 2g) was due to the intrusion of nutrient-rich open ocean water. Additionally, the observed DIN concentration in July was higher in the eastern part of the SIS, such as Osaka Bay, than in other regions, because the rivers with high DIN loads in the eastern area discharge more DIN into the SIS in summer. The observed DIN concentration was also high at the bottom layer of the central part of Harima Nada in May and July, due to the presence of bottom cold water there. The model reproduced the main seasonal variation and spatial distribution of DIN concentration in the SIS, except for the Bisan Strait and Osaka Bay, where the simulation results were lower than the observations. This was probably because the DIN loads from sewage sources were not considered in the model. The comparison of simulated DIN concentration versus observations suggests that the model works well in the areas with low concentrations (<10 $mmol\ m^{-3}$) but underestimates the high concentrations in some nearshore areas. Their linear correlation coefficient was 0.71 (Fig. 2i).

At the surface layer, the observed PHY concentration was high in May and October, with values over 1 $mg\ Chla\ m^{-3}$ (Fig. 3b, 3d). At the bottom layer, the observed PHY concentration remained at a low value below 0.5 $mg\ Chla\ m^{-3}$ all year round in most areas (Fig. 3e-3h). However, it was high in the nearshore areas, particularly around the estuaries. In January, the

https://doi.org/10.5194/egusphere-2023-753
Preprint. Discussion started: 2 May 2023

observed PHY concentration was similar between the surface and bottom layers (Fig. 3a, 3e). The difference in PHY concentration between the surface and bottom layers was larger in the simulation than in the observation. The simulated PHY concentration was lower than the observations in the nearshore areas. The comparison of simulated PHY concentration versus observations suggests that the model works well in areas with low concentrations (< 5 $mg\ Chla\ m^{-3}$) but underestimates the high concentrations in the nearshore areas. Their linear correlation coefficient was 0.63 (Fig. 3i).

It should be noted that the underestimations for DIN and PHY occur only in the nearshore areas (surface salinity < 30.6 in July refer to Ministry of the Environment, Japan), whose volume shares 5% of the whole SIS. In other words, the model can reproduce the seasonal variations and the spatial distribution of DIN and PHY in the other 95% volume of the SIS, which is sufficient for our purpose to examine the impacts of oceanic nutrients on the inventories of DIN and PHY in the SIS.

https://doi.org/10.5194/egusphere-2023-753
Preprint. Discussion started: 2 May 2023

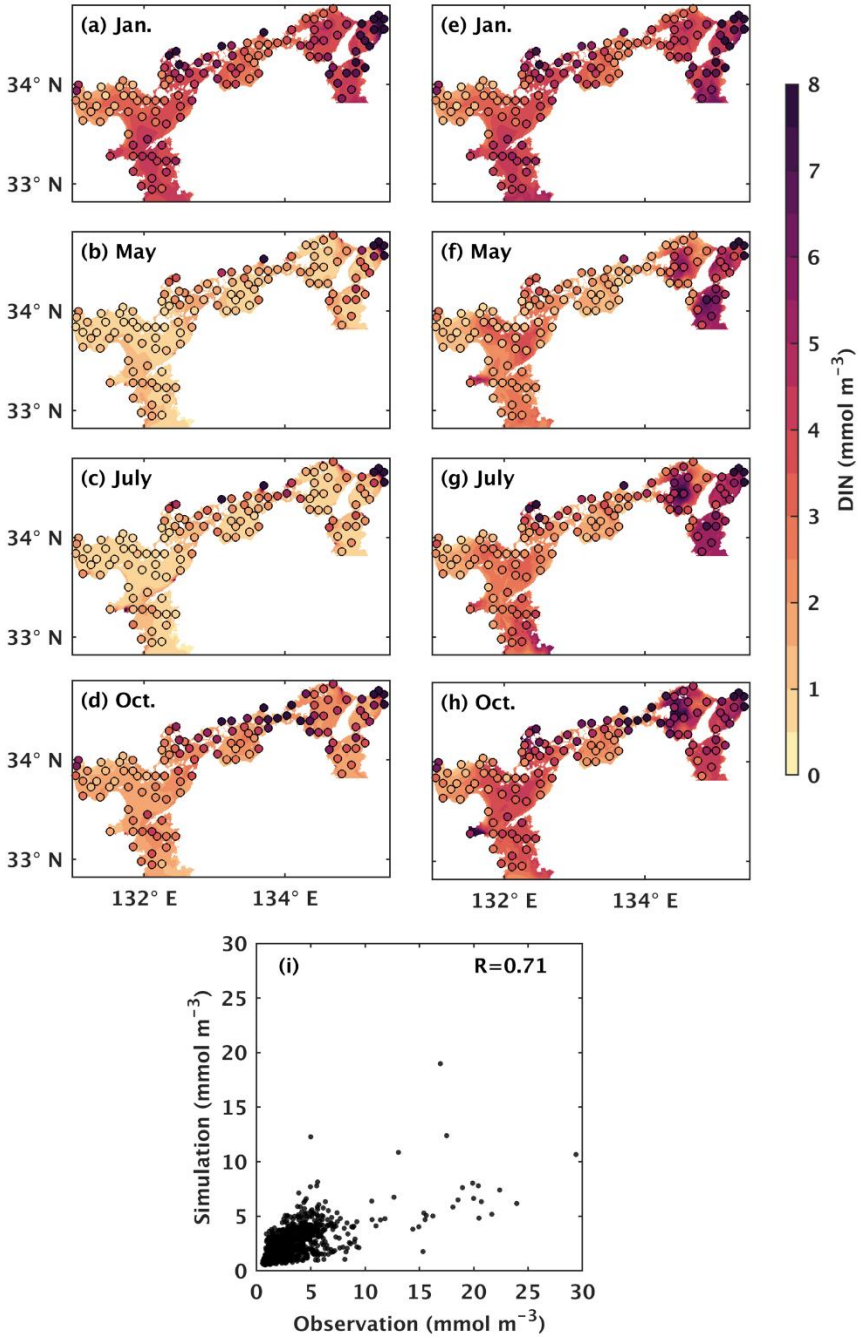

Figure 2. Monthly mean DIN concentration ($mmol\ m^{-3}$) at the **(a-d)** surface and the **(e-h)** bottom. Solid circles represent the observed values, and the background colour represents the simulation values. **(i)** Comparison between observed DIN concentrations versus simulated DIN concentrations.

https://doi.org/10.5194/egusphere-2023-753
Preprint. Discussion started: 2 May 2023

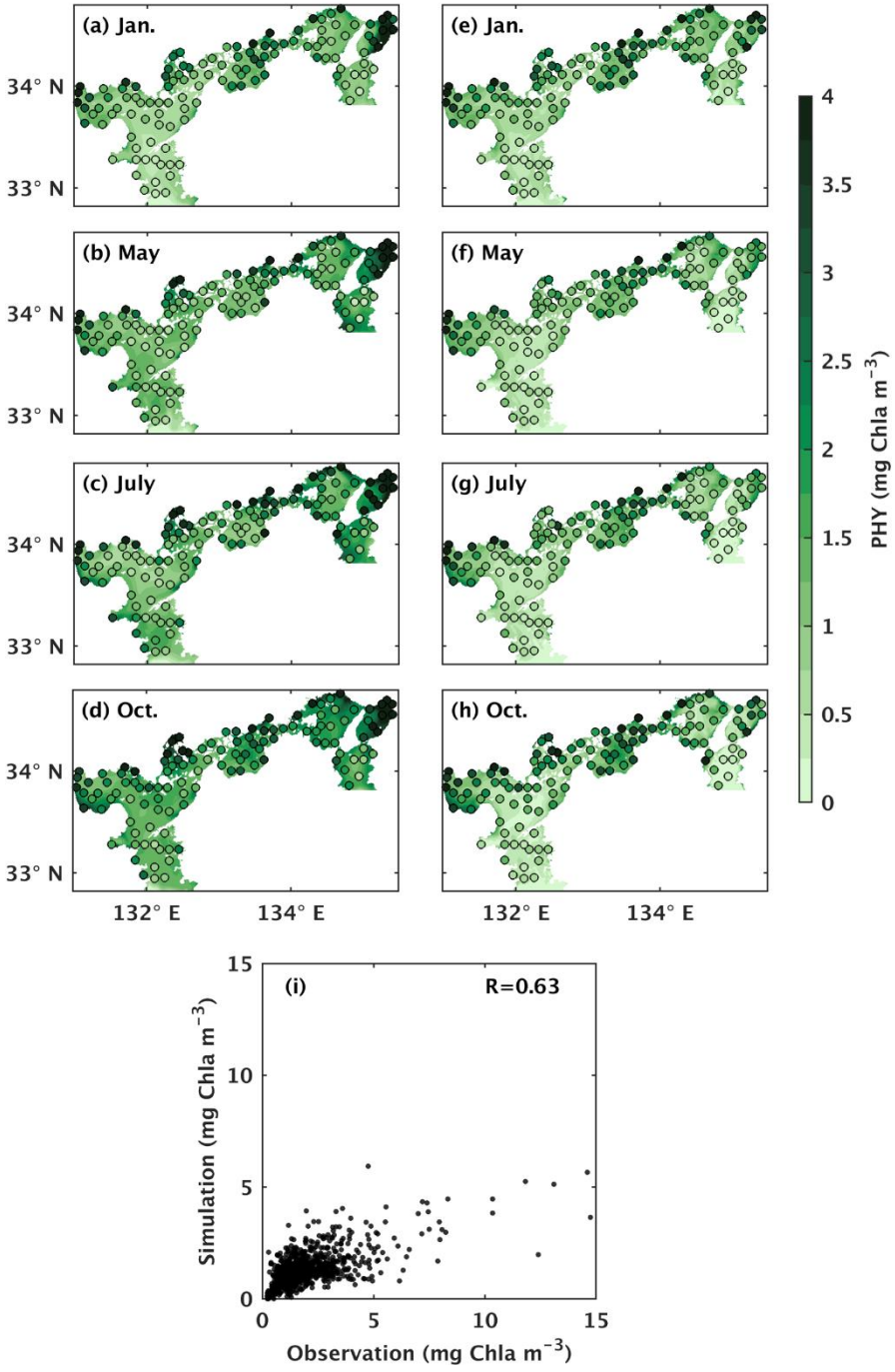

Figure 3. Monthly mean PHY concentration ($mg\ Chla\ m^{-3}$) at the **(a-d)** surface and the **(e-h)** bottom. Solid circles represent the observed values, and the background colour represents the simulation values. **(i)** Comparison between observed PHY concentrations versus simulated PHY concentration.

https://doi.org/10.5194/egusphere-2023-753
Preprint. Discussion started: 2 May 2023

3.2 Distribution of oceanic, riverine, and benthic DIN in the first year of simulations

The materials related to the DIN originating from the open ocean, rivers, and sediment were all set to zero at the initial stage of the simulation. After DIN loads were transported into the SIS, DIN concentration from each nutrient source gradually increased in the SIS until reaching the steady state of the annual cycle. The water-column averaged DIN concentration in the first year of tracking simulation was used to exhibit the pathway of DIN from each nutrient source into the SIS (Fig. 4).

The oceanic DIN intruded into the SIS from the Bungo Channel and Kii Channel and then entered the Iyo Nada and Osaka Bay. Gradually, it arrived the Suo Nada, Aki Nada, and Harima Nada. In the western part of the SIS, the oceanic DIN continued to intrude into Hiroshima Bay and Hiuchi Nada. On the other hand, in the eastern part of the SIS, the oceanic DIN was mainly concentrated at Kii Channel, Osaka Bay, and Harima Nada, but its concentration increased (Fig. 4a-4f). The oceanic DIN concentration at Bisan Strait started to increase at the end of the first year. On the other hand, the riverine DIN intruded into the SIS from the estuaries, especially in Osaka Bay and Harima Nada (Fig. 4g-4l). The benthic DIN concentration increased from the nearshore areas of Suo Nada, Hiroshima Bay, Hiuchi Nada, Harima Nada, and Osaka Bay (Fig. 4m-4p).

After one year of simulation, DIN concentrations from the open ocean, rivers, and sediment have already occupied most areas of the SIS. We used the results in the third year of the tracking simulation, which has reached the steady state of the annual cycle, for the following sections.

https://doi.org/10.5194/egusphere-2023-753
Preprint. Discussion started: 2 May 2023

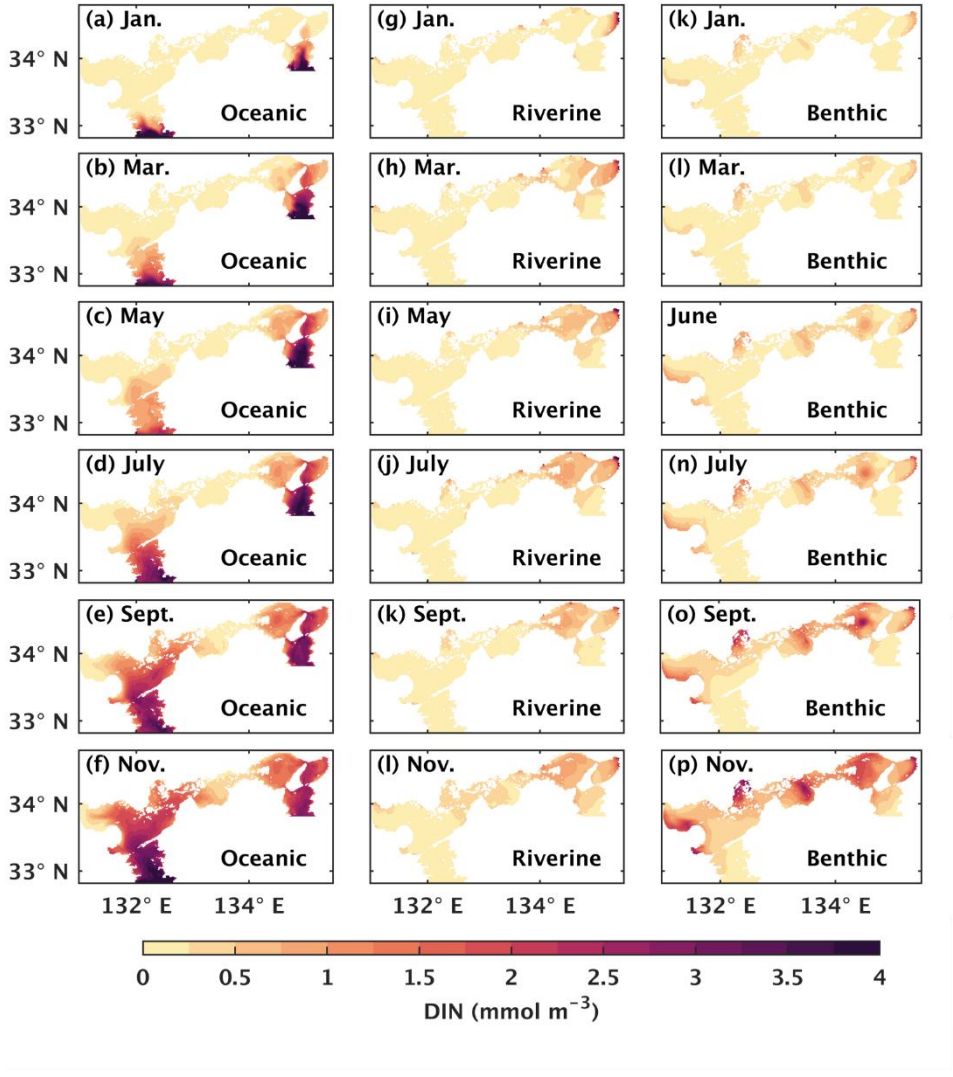

Figure 4. The water column averaged DIN concentration ($mmol\ m^{-3}$) from the open ocean, rivers, and sediment in the first year of the tracking simulation.

3.3 Contribution of different nutrient sources to DIN and PHY

The oceanic DIN concentration in the entire SIS showed a significant seasonal variation, with a decrease from 2.7 $mmol\ m^{-3}$ in January to 1.6 $mmol\ m^{-3}$ in June, followed by an increase until December, similar to the total DIN concentration (Fig. 5h). The proportion of oceanic DIN to the total DIN did not show an obvious seasonal variation, ranging between 70% and 80%, with an annual mean of 72% (Fig. 5i). The riverine and benthic DIN concentrations were much smaller than oceanic DIN concentration and remained around 0.28 $mmol\ m^{-3}$ and 0.52 $mmol\ m^{-3}$, respectively. The annual average contribution of riverine and oceanic sources to DIN concentration was 10% and 17%, respectively.

https://doi.org/10.5194/egusphere-2023-753
Preprint. Discussion started: 2 May 2023

Regarding the annual mean spatial variation, the oceanic DIN concentration averaged over the entire depth was higher than 2.5 $mmol\ m^{-3}$ in the Bungo Channel and Kii Channel, while it was lower than 0.5 $mmol\ m^{-3}$ in Bisan Strait and Bingo Nada (Fig. 5b). The oceanic contribution to DIN concentration decreased from the southern boundary areas to the inner part of the SIS and exhibited lower values in the nearshore areas. For different sub-regions, the proportion of oceanic nutrients was high at Bungo Channel (89%), Kii Channel (81%), and Iyo Nada (75%) and low at Bisan Strait (26%), Bingo Nada (28%) (Fig. 7a). The riverine concentration was highest in Harima Nada and Osaka Bay, due to large terrestrial input, and the corresponding contribution was also highest in these two sub-regions with a value of about 25%. The benthic concentration was higher in Bingo Nada, Harima Nada, and Hiroshima Bay, while its contribution was higher in Bingo Nada and Bisan Strait, with a value of about 55%.

The volume averaged PHY concentration supported by oceanic DIN also exhibited a significant seasonal variation, with an obvious spring bloom in March (0.64 $mg\ Chla\ m^{-3}$) (Fig. 6h). However, the seasonal variation in the oceanic contribution to the total PHY concentration remained close to the annual mean value of 60% (Fig. 6i). The PHY concentrations supported by riverine DIN and benthic DIN also change much with seasons, with an annual average of 0.14 $mg\ Chla\ m^{-3}$ and 0.22 $mg\ Chla\ m^{-3}$, respectively. The annual average contribution of riverine and benthic sources to PHY concentration was 15% and 25%, respectively.

For the spatial variation of annual mean, the oceanic PHY concentration averaged over the entire depth remained at 0.5 $mg\ Chla\ m^{-3}$ in most areas of the SIS (Fig. 6b). However, the oceanic contribution to PHY concentration exhibited an obvious spatial pattern, decreasing from the southern boundary areas into the inner part of the SIS and showing lower values in the nearshore areas, similar to DIN. For different sub-regions, the oceanic contribution was much higher at Bungo Channel (85%), Kii Channel (67%), and Iyo Nada (69%) and lower at Bisan Strait (25%), Bingo Nada (28%) (Fig. 7b). The riverine contribution was higher at Harima Nada (31%) and Osaka Bay (37%), while the benthic contribution was higher at Bingo Nada (56%) and Bisan Strait (48%).

https://doi.org/10.5194/egusphere-2023-753
Preprint. Discussion started: 2 May 2023

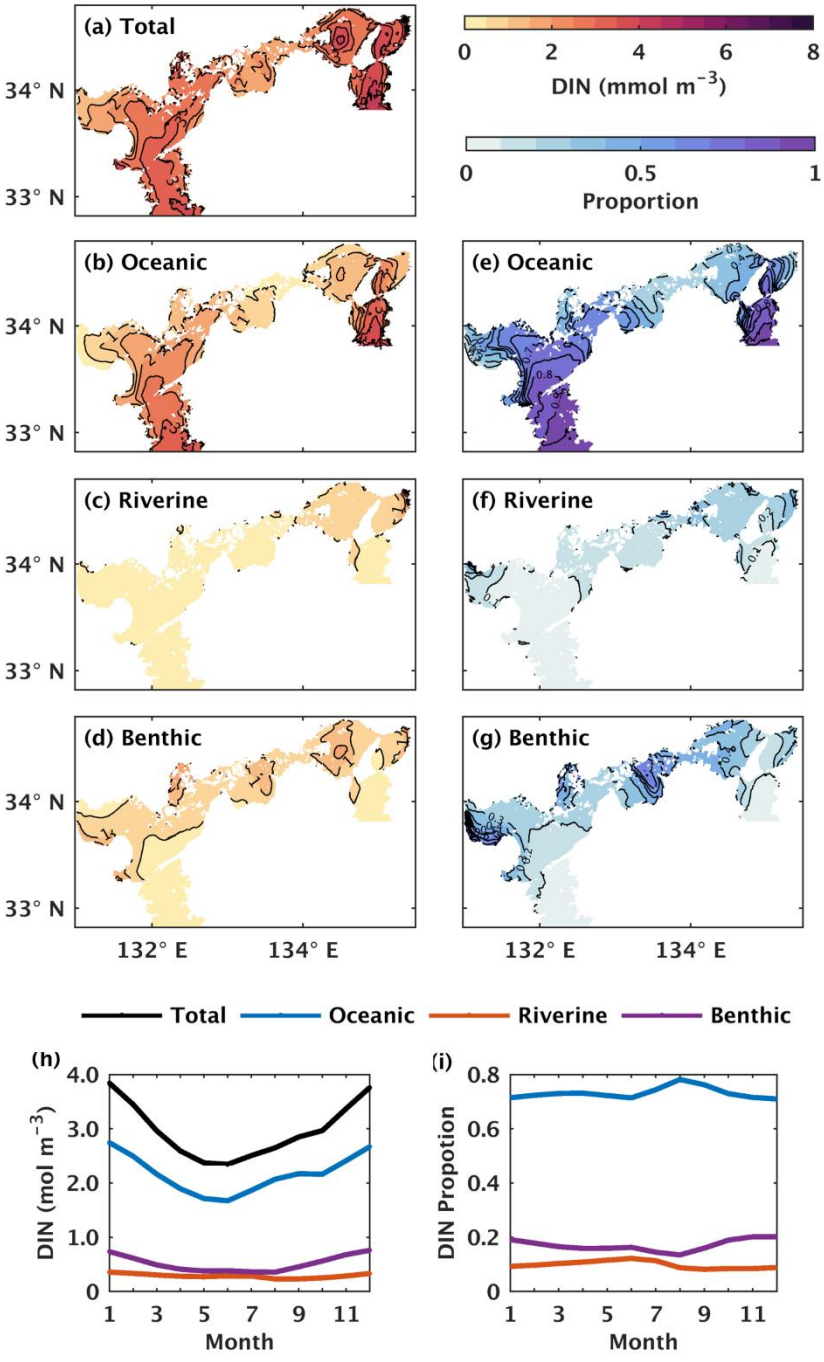

275 **Figure 5. (a-d)** The annual mean of water column-averaged DIN concentration ($mmol\ m^{-3}$) originating from the open ocean, rivers, and sediment. **(e-g)** Contributions of the open ocean, rivers, and sediment to total DIN concentration. **(h)** The monthly average oceanic, riverine, and benthic DIN concentration ($mmol\ m^{-3}$) in the whole SIS. **(i)** The monthly variations of oceanic, riverine, and benthic contributions to total DIN concentration in the whole SIS.

https://doi.org/10.5194/egusphere-2023-753
Preprint. Discussion started: 2 May 2023

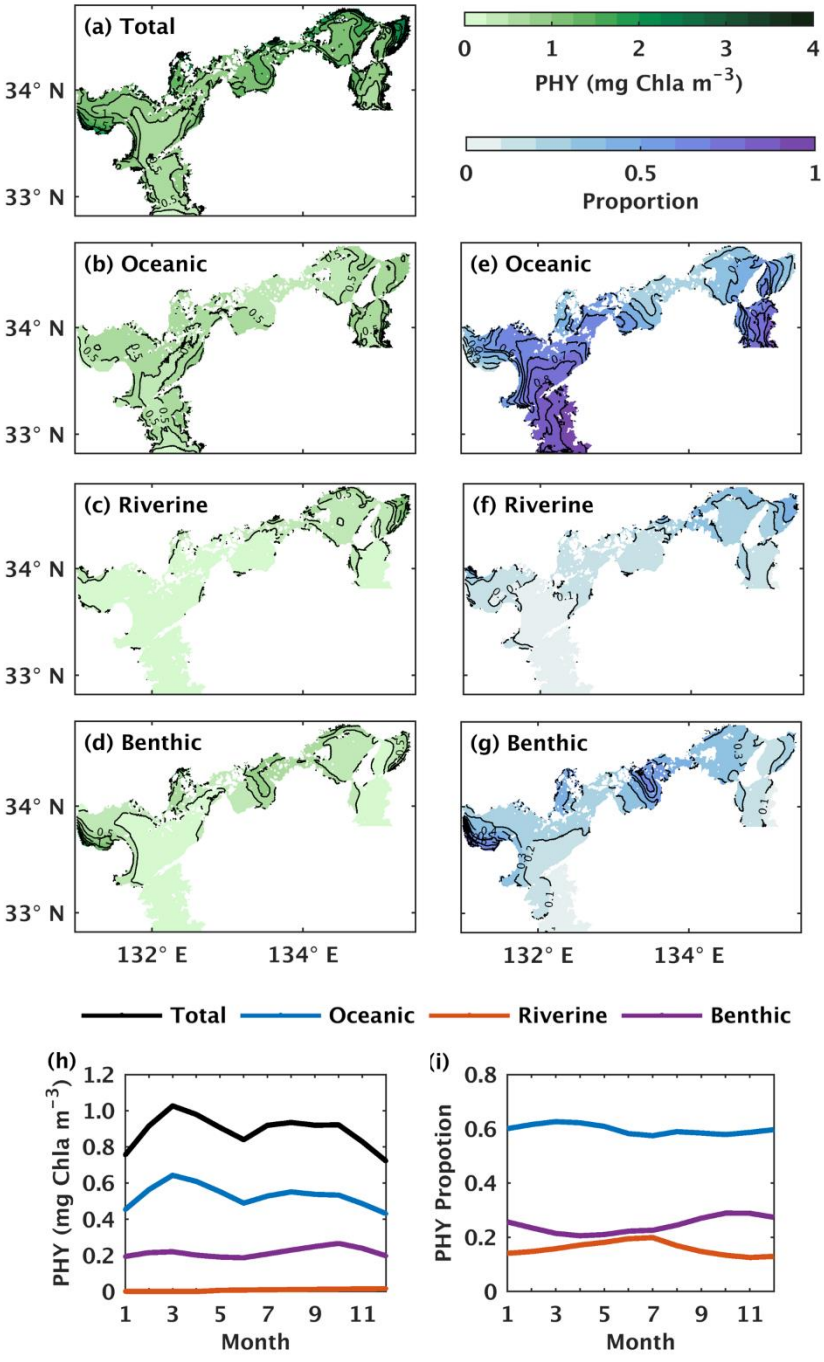

Figure 6. **(a-d)** The annual mean of water column-averaged PHY concentration ($mg\ Chla\ m^{-3}$) originating from the open ocean, rivers, and sediment. **(e-g)** Contributions of the open ocean, rivers, and sediment to total PHY concentration. **(h)** The monthly average oceanic, riverine, and benthic PHY concentration ($mg\ Chla\ m^{-3}$) in the whole SIS. **(i)** The monthly variations of oceanic, riverine, and benthic contributions to total PHY concentration in the whole SIS.

https://doi.org/10.5194/egusphere-2023-753
Preprint. Discussion started: 2 May 2023

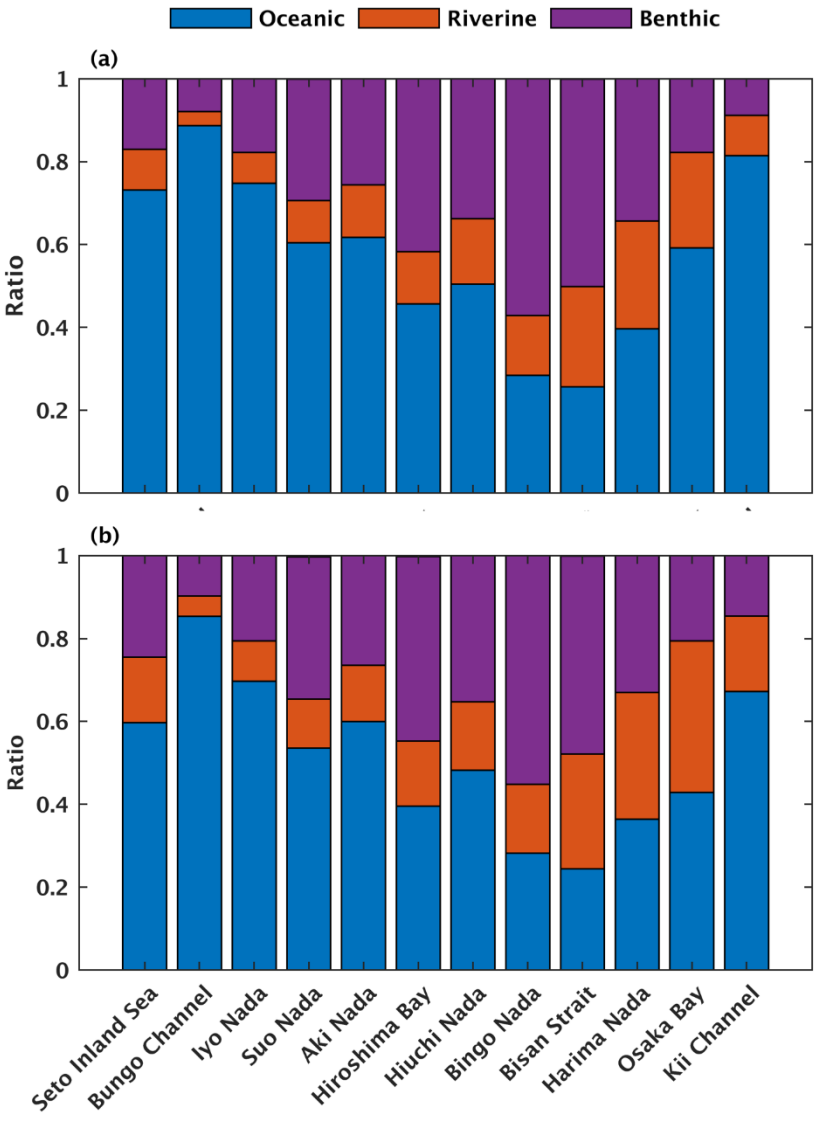

285 **Figure 7**. Contributions of the open ocean, rivers, and sediment to total **(a)** DIN and **(b)** PHY concentrations in sub-regions of SIS.

3.4 DIN transport across the boundary between SIS and open ocean

The oceanic DIN flux was primarily transported from the open ocean to the SIS at the lower layers, reflecting the intrusion of nutrient-rich Kuroshio subsurface water from the bottom, and out of the SIS at the upper layers and eastern part of the open
290 boundaries (Fig. S6). In terms of the seasonal variation of DIN transport at the Bungo Channel, the onshore transport of oceanic

https://doi.org/10.5194/egusphere-2023-753
Preprint. Discussion started: 2 May 2023

DIN was highest in January and July, with a value of 707 $mol\ s^{-1}$ and 664 $mol\ s^{-1}$ respectively, and lowest in April and May with a value of 236 $mol\ s^{-1}$ and 226 $mol\ s^{-1}$, respectively (Fig. 8a). There is also offshore transport of oceanic DIN across the open boundary. Its value was highest in January and February, with a value of -648 $mol\ s^{-1}$ and -550 $mol\ s^{-1}$, respectively, and lowest in April and May, with a value of -244 $mol\ s^{-1}$ and -215 $mol\ s^{-1}$, respectively. Consequently, the net oceanic DIN transport was highest in July and August, with a value of 275 $mol\ s^{-1}$ and 215 $mol\ s^{-1}$, respectively, and lowest in April and May, with a value of -8 $mol\ s^{-1}$ and 10 $mol\ s^{-1}$, respectively (Fig. 8a).

The seasonal variation of oceanic DIN transport across the Kii Channel was somewhat different from that of the Bungo Channel. The onshore transport of oceanic DIN was highest in July and August, with a value of 407 $mol\ s^{-1}$ and 483 $mol\ s^{-1}$, respectively, and lowest in April and May, with a value of 199 $mol\ s^{-1}$ and 215 $mol\ s^{-1}$, respectively. The offshore transport of oceanic DIN was highest in July and August, with a value of -277 $mol\ s^{-1}$ and -329 $mol\ s^{-1}$, respectively, and lowest in March and April, with a value of -123 $mol\ s^{-1}$ and -112 $mol\ s^{-1}$, respectively. Consequently, the net oceanic DIN transport was highest in July and August, with a value of 130 $mol\ s^{-1}$ and 154 $mol\ s^{-1}$, respectively, and lowest in May and November, with a value of 70 $mol\ s^{-1}$ and 67 $mol\ s^{-1}$, respectively (Fig. 8b).

The onshore transport of oceanic DIN has an annual mean of 505 $mol\ s^{-1}$ at Bungo Channel and 292 $mol\ s^{-1}$ at Kii Channel, whose sum is 797 $mol\ s^{-1}$. The offshore transport of oceanic DIN has an annual mean of -394 $mol\ s^{-1}$ at Bungo Channel and of -198 $mol\ s^{-1}$ at Kii Channel, whose sum is -592 $mol\ s^{-1}$. The values produce an annual mean of net oceanic DIN transport of 111 $mol\ s^{-1}$ at Bungo Channel and 96 $mol\ s^{-1}$ at Kii Channel, whose sum is 205 $mol\ s^{-1}$.

https://doi.org/10.5194/egusphere-2023-753
Preprint. Discussion started: 2 May 2023

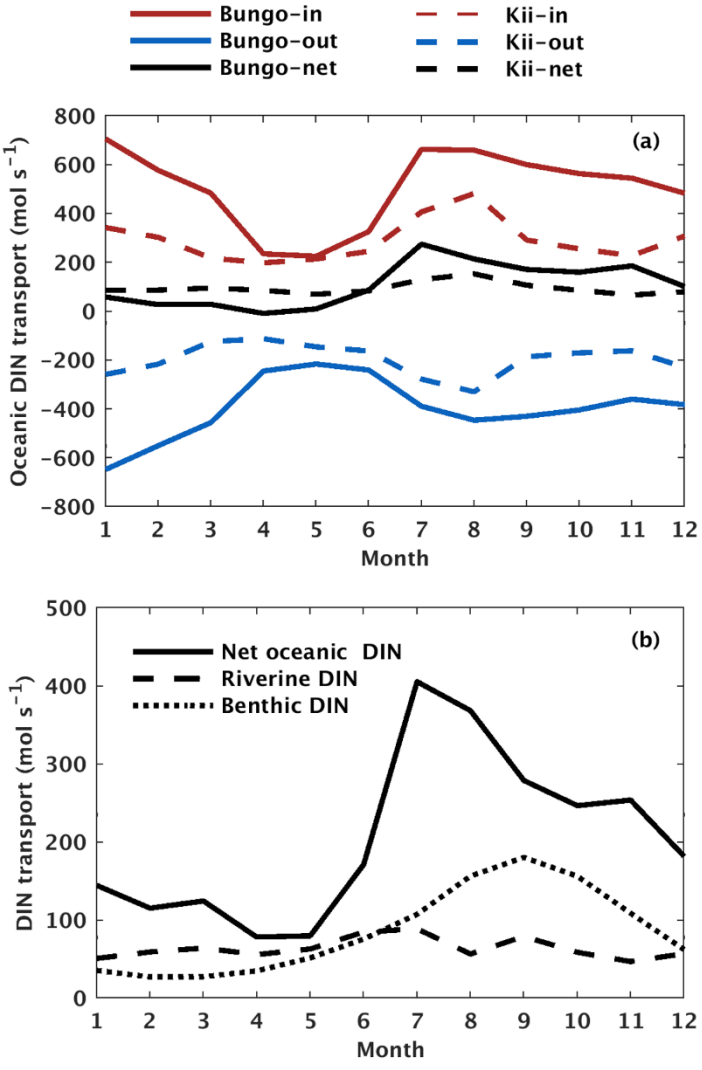

Figure 8. **(a)** Monthly variation of onshore, offshore, and net transport of ocean DIN ($mol\ s^{-1}$) across the Bungo Channel and Kii Channel. **(b)** Monthly variation of DIN loads ($mol\ s^{-1}$) from the open ocean, rivers, and sediment.

4 Discussion

4.1 Role of open ocean in DIN inventory of different shelf seas

Our simulation reveals that the annual mean inventory of DIN in the whole SIS was $26.0 \times 10^8\ mol$, among which that originating from the open ocean, rivers, and sediment was 18.9×10^8, 2.54×10^8, and $4.57 \times 10^8\ mol$, respectively, sharing a proportion of 73%, 10%, and 17%, respectively (Fig. 9). The oceanic contribution to DIN inventory in our simulation (73%)

https://doi.org/10.5194/egusphere-2023-753
Preprint. Discussion started: 2 May 2023

was close but less than 81% proposed by (Yanagi and Ishii, 2004) who did not consider biogeochemical processes and nutrient release from sediment.

In terms of PHY, the annual mean inventory supported by DIN from the open ocean, rivers, and sediment was 2.95×10^8, 0.79×10^8, and 1.21×10^8 $mol\ N$, respectively, which imply a proportion of 60%, 15%, and 25%, respectively, in the whole inventory (Fig. 9). Although being smaller than the contribution to DIN, the open ocean is still a dominant contributor to PHY in the SIS. If we consider the total nitrogen, which is defined as the sum of DIN, PHY, ZOO, and PON in this study, the open ocean contributes 67% to its inventory in the SIS.

In the ECS, a marginal sea in the Northwest Pacific Ocean with a broad continental shelf, the open ocean plays a dominant role in areas shallower than 200 m, contributing 57% of the DIN inventory (Zhang et al., 2019). Even though the ECS is more open to the open ocean, our simulation showed that the open ocean contributed more to the DIN inventory in the SIS compared to the ECS. In a shallow estuary located on the east coast of Jutland, Denmark, which is well-ventilated with the open ocean, the open ocean contributed less than 40% to the DIN inventory in most areas of the estuary (Timmermann et al., 2010). In the Northern Gulf of Mexico, another marginal sea receiving large amounts of nutrients from rivers, the open ocean contributed less than 15% of the total nitrogen inventory in the shallow regions, where rivers contribute more than 85% (Große et al., 2019). Our study also found that the open ocean contributed less than 30% in the nearshore areas with shallow water depth and large riverine nutrient inputs (Fig. 5c). Apparently, the oceanic contribution to the nutrient inventory in these water bodies varies largely and should strongly depend on its cycling rate in the low-trophic system of the shelf sea.

4.2 DIN and PHY material flows

To understand the different proportions of oceanic, riverine, and benthic nutrients in the inventory of DIN in the SIS, we present its related material flows here (Fig. 9).

The annual mean budget flows of DIN in the SIS can be described using Eq. (6), where the amount of DIN delivered to the SIS from external sources is equal to the sum of the amount consumed by biogeochemical processes that transfer DIN to the biological particles and the amount exported to the open ocean through open boundaries in the form of DIN.

$$Input\ transport = Output\ amount + Net\ biogeochemical\ processes\ of\ DIN, \quad (6)$$

$$Net\ biogeochemical\ processes\ of\ DIN = -Photosynthesis + Respiration + Mineralization + Excretion, \quad (7)$$

Our study found that the input amount of DIN from the open ocean, rivers, and sediment was 799, 64, and 86 $mol\ s^{-1}$, respectively, with a ratio of 84%, 7%, and 9%. The output amount of oceanic, riverine, and benthic DIN to the open ocean was -594, -14, and -17 $mol\ s^{-1}$, respectively, with a ratio of 95%, 2%, and 3%. The net biogeochemical process of DIN from the open ocean, rivers, and sediment was -205, -50, and -69 $mol\ s^{-1}$, respectively, with a ratio of 63%, 15%, and 22%. These results indicate that only 25% of the input oceanic DIN was involved in biogeochemical processes, and 75% was returned to the open ocean (Fig. 9a). Therefore, the role of oceanic nutrients may be overestimated in terms of the input amount. In contrast,

https://doi.org/10.5194/egusphere-2023-753
Preprint. Discussion started: 2 May 2023

riverine and benthic DIN inputs transport was smaller than oceanic DIN, but 78% and 80% of their inputs were involved in biogeochemical processes, indicating more bioactive effects (Fig. 9b, 9c).

In the North Sea, which is a semi-enclosed sea connected to North Atlantic Ocean through its northern boundary, the open ocean contributed 75% of the total nitrogen budget in the north open area (Vermaat et al., 2008). Similarly, in the ECS, the open ocean contributed 72% of the DIN input amount in areas shallower than 200 m (Zhang et al., 2019). As shown by Zhang et al. (2019), the contribution of oceanic DIN to primary production in the ECS is lower than the proportions of DIN input (72%). Such a difference suggests a different efficiency of DIN with different origins.

In our simulation, we did not allow external sources to bring PHY into the SIS through open boundaries. Therefore, the PHY generated through biogeochemical processes inside the SIS was transported to the open ocean through the open boundaries. The equation governing the budget of PHY is represented by Eq. (8). The net biogeochemical processes of PHY are defined in Eq. (9)

$$0 = Output\ transport + Net\ biogeochemical\ processes\ of\ PHY, \quad (8)$$

$$Net\ biogeochemical\ processes\ of\ PHY = Photosynthesis - Respiration - Grazing - Mortality, \quad (9)$$

The oceanic proportion of photosynthesis was 56%, which is lower than the proportion of oceanic DIN in the total inventory. This may be due to the fact that the oceanic DIN was primarily distributed in the bottom layer of areas with deep depth in the SIS (Fig. 5b). As a result, some of the oceanic DIN in the deep layer may not be available for photosynthesis due to light limitation, leading to a lower proportion of oceanic photosynthesis compared to oceanic DIN. In contrast, riverine and benthic DIN were mainly distributed in the areas with shallow depths where the light condition is good (Fig. 5c, 5d).

The net biogeochemical process of PHY defined by Eq. (9) was 66, 7, and 7 $mol\ s^{-1}$ for the oceanic riverine, and benthic DIN, respectively, which are exactly the same as the output amount of PHY from the open boundaries. Their ratio of 82%, 9%, and 9% suggests that the oceanic PHY was more likely to leave the SIS.

The inventory of ZOO and PON depends on that of PHY and consequently the nutrients from the open ocean support more than half of ZOO and PON in the SIS. The export of biological particles from SIS is important for a material balance in the sea. In the SIS, the horizontal export flux of biological particles (PHY+ZOO+PON) to the open ocean is 187 $mol\ s^{-1}$ (Fig. 9a) and the vertical export flux of biological particles to the sediment is 136 mol s^{-1}, whose ratio is 1.4:1. If we examine them for the different origin of nutrients, this ratio changes. For oceanic nutrients (Fig. 9b), the horizontal export of biological particles has a flux of 142 $mol\ s^{-1}$ while the vertical export has a value of 62 $mol\ s^{-1}$, whose ratio is 2.3:1; for the riverine nutrients (Fig. 9c), the horizontal export has a flux of 23 $mol\ s^{-1}$ while the vertical export has a value of 27 mol s^{-1}, whose ratio is 0.85:1; for the benthic nutrients (Fig. 9d), the horizontal export has a flux of 22 $mol\ s^{-1}$ while the vertical export has a value of 47 mol s^{-1}, whose ratio is 0.48:1. Considering the spatial distribution of these different origins of nutrients, the difference in ratios is likely a natural result of water exchange between the SIS and open ocean.

https://doi.org/10.5194/egusphere-2023-753
Preprint. Discussion started: 2 May 2023

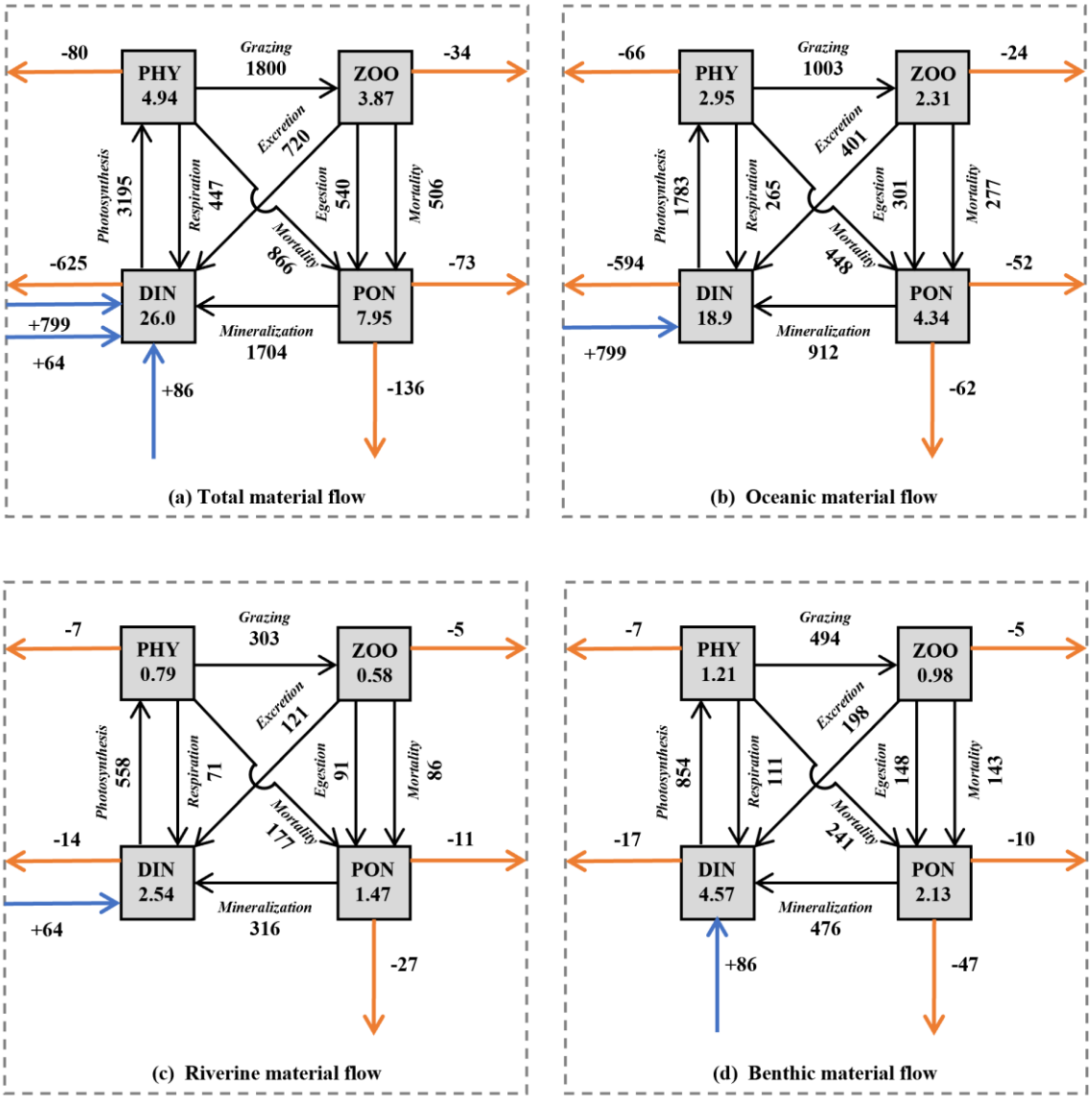

Figure 9. The annual mean of material inventories and material flows in the whole SIS. **(a)** Total inventories and material flows **(b)** Oceanic inventories and material flows **(c)** Riverine inventories and material flows **(d)** Benthic inventories and material flows. The values in the rectangles represent the inventory ($\times 10^8\ mol$) of each material in the SIS. The values next to the black solid lines with an arrow represent the flux of biogeochemical processes ($mol\ s^{-1}$). The values next to the horizontal orange solid lines with an arrow represent the horizontal flux from the SIS to the open ocean ($mol\ s^{-1}$). The values next to the vertical orange solid lines with an arrow represent the vertical flux to the sediment ($mol\ s^{-1}$). The values next to the blue solid line with a vertical arrow represent the flux of benthic DIN into the SIS.

https://doi.org/10.5194/egusphere-2023-753
Preprint. Discussion started: 2 May 2023

4.3 Response of the SIS to changes in nutrient input

Understanding the response of SIS to changes in nutrient inputs from different nutrient sources is crucial for effective nutrient management. To investigate this, we conducted sensitivity experiments by varying the input amount of each nutrient source individually. Nutrient inputs were altered by adding or subtracting the standard deviation of long-term variation of nutrient input based on the climatological input amount. This allowed us to simulate the responses of SIS to the larger and smaller inputs that may occur.

For the DIN load from rivers, we added twice the standard deviation to the climatological value for the upper limit but removed only one standard deviation from the climatological value for the lower limit to avoid negative values. The upper limit situation was to account for the high amount of nutrient load from the land during the high economic development period in Japan. The variation of DIN loads from rivers was specified in the model by changing the nutrient concentration in river water to avoid changes in the hydrodynamic fields due to the change in river discharge. For DIN load from the open ocean, the nutrient concentration at the open boundaries was added or minus one standard deviation to obtain the upper limit or lower limit, and the open boundary conditions for the hydrodynamic model were not changed. For DIN load from the sediment, TN concentration at the sediment surface in the 1980s was selected as the upper limit and TN concentration in the 2010s was selected as the lower limit because the TN data in the 1980s, 1990s, 2000s, and 2010s show a reduction trend throughout these years. Table 1 summarized the input amount of DIN from the open ocean, rivers, and sediment in each sensitivity experiment.

Table 1. Annual mean input amount of DIN ($mol\ s^{-1}$) from the open ocean, rivers, and sediment in sensitivity experiments. "L" means the lower limit case; "U" means the upper limit case. The percentages mean the relative change from the value in the control case.

Name of cases	**From rivers**	**From open ocean**	**From sediment**	**Total input**
Control	64	799	86	949
L-open ocean	64	527 (-34%)	86	677 (-29%)
U-open ocean	64	1073 (+34%)	86	1223(+29%)
L-rivers	43 (-33%)	799	86	928 (-2.2%)
U-rivers	105 (+64%)	799	86	990 (+4.3%)
L-sediment	64	799	60 (+30%)	923 (-2.7%)
U-sediment	64	799	136 (+58%)	999 (+5.2%)

When the DIN load from the open ocean was reduced by 34% (case of L-open ocean in Table 1), there was a corresponding decrease in the concentration of oceanic DIN by 34% ((1.41-2.13)/2.13), as well as a decrease in the concentration of oceanic PHY by 28% ((0.38-0.53)/0.53) (Table 2). As a result, the contribution of oceanic DIN and PHY to the total concentration

https://doi.org/10.5194/egusphere-2023-753
Preprint. Discussion started: 2 May 2023

decreased by 10%, while those of riverine and benthic DIN and PHY increased with a range between 3% to 6%. Conversely, when the DIN load from the open ocean was increased by 34% (case of U-open ocean in Table 1), the concentration of oceanic DIN increased by 35%, and that of oceanic PHY by 25% (Table 2). Then, the contribution of oceanic DIN and PHY to the total concentration increased by 5%, while that of riverine and benthic DIN and PHY decreased by 3%.

Similarly, when the DIN load from rivers was reduced by 34% (case of L-rivers), the concentration of riverine DIN and PHY decreased by 28%, and their contribution to the total concentration decreased by 3% (Table 2). On the other hand, when the DIN load from rivers was increased by 64% (case of U-rivers), the concentration of riverine DIN and PHY increased by 50% and 55%, respectively, and their contribution to the total concentration increased by 5% and 7%, respectively. In these two cases, the contribution of oceanic and benthic DIN and PHY changed with a range of less than 5%.

When the DIN load from the sediment was reduced by 30% (case of L-sediment), the concentration of benthic DIN and PHY decreased by about 20%, and their contribution to the total concentration decreased by about 4%. When the DIN load from the sediment was increased by 58% (case of U-sediment), the concentration of benthic DIN and PHY increased by 29% and 23%, respectively, and their contribution to the total concentration increased.

Overall, the change in the DIN load from a specific nutrient source led to the same order change in the corresponding DIN and PHY concentrations, but a small range of change in the contribution of all nutrient sources. Specifically, despite significant changes in DIN loads from rivers and sediment, their contribution to the SIS was only minimally impacted due to their low proportion. This can be understood by the relative change in the inventory of total DIN and total PHY in Table 2. In these experiments, the changes in oceanic nutrients can cause more than 20% change in total DIN inventory and more than 10% change in PHY inventory. However, the changes in riverine nutrients or benthic nutrients can cause only ~5% changes in the total DIN inventory and PHY inventory.

https://doi.org/10.5194/egusphere-2023-753
Preprint. Discussion started: 2 May 2023

Table 2. Annual mean oceanic, riverine, and benthic DIN concentration ($mmol\ m^{-3}$) and PHY concentration ($mg\ Chla\ m^{-3}$) and their proportion in total DIN and PHY concentration in the entire SIS in the sensitivity experiments. The percentage in column 6 is the relative change to the values in the case of "Control".

Name		**Oceanic**	**Riverine**	**Benthic**	**Total**
Control	DIN	2.13 (73%)	0.29 (10%)	0.51 (17%)	2.93
	PHY	0.53 (60%)	0.14 (16%)	0.22 (24%)	0.89
L-open ocean	DIN	1.41 (64%)	0.29 (13%)	0.52 (23%)	2.22 (-24%)
	PHY	0.38 (50%)	0.15 (20%)	0.23 (30%)	0.76 (-15%)
U-open ocean	DIN	2.87 (78%)	0.29 (8%)	0.52 (14%)	3.68 (+26%)
	PHY	0.66 (66%)	0.13 (13%)	0.21 (21%)	1.00 (+12%)
L-rivers	DIN	2.13 (75%)	0.21 (7%)	0.52 (18%)	2.86 (-2.4%)
	PHY	0.53 (62%)	0.10 (12%)	0.22 (26%)	0.85 (-4.5%)
U-rivers	DIN	2.13 (69%)	0.45 (15%)	0.53 (16%)	3.11 (+6.1%)
	PHY	0.52 (55%)	0.21 (23%)	0.21 (22%)	0.94 (+5.6%)
L-sediment	DIN	2.13 (75%)	0.29 (10%)	0.41 (15%)	2.83 (-3.4%)
	PHY	0.53 (63%)	0.14 (17%)	0.17 (20%)	0.84 (-5.6%)
U-sediment	DIN	2.13 (69%)	0.29 (9%)	0.66 (21%)	3.08 (+5.1%)
	PHY	0.52 (56%)	0.14 (15%)	0.27 (29%)	0.93 (+4.5%)

https://doi.org/10.5194/egusphere-2023-753
Preprint. Discussion started: 2 May 2023

5 Conclusions

In this study, we investigate the behaviours of oceanic, riverine, and benthic nutrients to the inventory of nutrients and phytoplankton in the SIS using a low-trophic model with an embedded tracking module. Our study shows the largest contribution of oceanic nutrients to the inventory of nutrients and phytoplankton in the SIS and its lowest efficiency in the primary production in the SIS. On the other hand, although the riverine or benthic nutrients have a lower contribution to the inventory of nutrients and phytoplankton in the SIS than the oceanic nutrients do, they demonstrate a higher efficiency in the primary production in the SIS. It must be noted that their contributions have a strong spatial variation, in which the oceanic nutrients range from > 90% in the area close to the open ocean to < 30% in the nearshore areas, while the riverine or benthic nutrients range from >50% in the nearshore areas to <10% in the areas far from the estuaries and inner bays.

The above results give us several hints for the management strategy for the SIS. Firstly, the oceanic nutrients provide a background of nutrients that supports the primary production in the SIS, and it can cause a temporal variation with a range of 20% in the inventory of nutrients and phytoplankton. This part of nutrients is mainly controlled by the variations in the nutrient concentration in the open ocean and the water exchange between the SIS and open ocean and human-made management on nutrient load from land cannot affect this part of nutrients. Secondly, the management should be easily applied to the riverine nutrients whose impact has a strong spatial distribution. Therefore, the target of management should be carefully examined to confirm the local impacts of each river before the determination of the management plan. Thirdly, although it is a little difficult, the management can also be applied to the sediments, because its impacts are larger than those of riverine nutrients in some places.

Code availability

The source code of the numerical model used in this study is available on request. Please contact the corresponding author.

Author contribution

JZ developed the hydrodynamic model. AM developed the low-trophic model. QL combined two models and introduced the tracking module into them. QL and XG prepared the manuscript. All the authors reviewed the manuscript.

Competing interests

The authors declare that they have no conflict of interest.

https://doi.org/10.5194/egusphere-2023-753
Preprint. Discussion started: 2 May 2023

Acknowledgements

This research was performed by the Environment Research and Technology Development Fund (JPMEERF20205005) of the Environmental Restoration and Conservation Agency Provided by the Ministry of Environment of Japan. We thank Dr. Yoshitsugu Koizumi who worked in the Fisheries Research Center, Ehime Prefectural Institute of Agriculture, Forestry and Fisheries, Japan and provided us with the observed nutrients and water temperature data in the Bungo Channel.

References

Abo, K. and Yamamoto, T.: Oligotrophication and its measures in the Seto Inland Sea, Japan, Bull. Jpn. Fish. Res. Educ. Agency, 49, 21–26, 2019.

Anderson, D. M., Burkholder, J. M., Cochlan, W. P., Glibert, P. M., Gobler, C. J., Heil, C. A., Kudela, R. M., Parsons, M. L., Rensel, J. E. J., Townsend, D. W., Trainer, V. L., and Vargo, G. A.: Harmful algal blooms and eutrophication: Examining linkages from selected coastal regions of the United States, Harmful Algae, 8, 39–53, https://doi.org/10.1016/j.hal.2008.08.017, 2008.

Aoki, K., Shimizu, Y., Yamamoto, T., Yokouchi, K., Kishi, K., Akada, H., and Kurogi, H.: Estimation of inward nutrient flux from offshore into semi-enclosed sea (Tokyo Bay, Japan) based on in-situ data, Estuar. Coast. Shelf Sci., 274, 107930, https://doi.org/10.1016/j.ecss.2022.107930, 2022.

Bauer, J. E., Cai, W.-J., Raymond, P. A., Bianchi, T. S., Hopkinson, C. S., and Regnier, P. A. G.: The changing carbon cycle of the coastal ocean, Nature, 504, 61–70, https://doi.org/10.1038/nature12857, 2013.

Blumberg, A. F. and Mellor, G. L.: A description of a three-dimensional coastal ocean circulation model, in: Coastal and Estuarine Sciences, vol. 4, edited by: Heaps, N. S., American Geophysical Union, Washington, D. C., 1–16, https://doi.org/10.1029/CO004p0001, 1987.

Caddy, J.: Marine catchment basin effects versus impacts of fisheries on semi-enclosed seas, ICES J. Mar. Sci., 57, 628–640, https://doi.org/10.1006/jmsc.2000.0739, 2000.

Chang, P.-H., Guo, X., and Takeoka, H.: A numerical study of the seasonal circulation in the Seto Inland Sea, Japan, J. Oceanogr., 65, 721–736, https://doi.org/10.1007/s10872-009-0062-4, 2009.

Fasham, M. J. R., Ducklow, H. W., and McKelvie, S. M.: A nitrogen-based model of plankton dynamics in the oceanic mixed layer, J. Mar. Res., 48, 591–639, https://doi.org/10.1357/002224090784984678, 1990.

Fennel, K., Wilkin, J., Levin, J., Moisan, J., O'Reilly, J., and Haidvogel, D.: Nitrogen cycling in the Middle Atlantic Bight: Results from a three-dimensional model and implications for the North Atlantic nitrogen budget: NITROGEN CYCLING IN THE MIDDLE ATLANTIC, Glob. Biogeochem. Cycles, 20, n/a-n/a, https://doi.org/10.1029/2005GB002456, 2006.

Große, F., Fennel, K., and Laurent, A.: Quantifying the Relative Importance of Riverine and Open-Ocean Nitrogen Sources for Hypoxia Formation in the Northern Gulf of Mexico, J. Geophys. Res. Oceans, 124, 5451–5467, https://doi.org/10.1029/2019JC015230, 2019.

https://doi.org/10.5194/egusphere-2023-753
Preprint. Discussion started: 2 May 2023

Guo, X., Futamura, A., and Takeoka, H.: Residual currents in a semi-enclosed bay of the Seto Inland Sea, Japan, J. Geophys. Res., 109, C12008, https://doi.org/10.1029/2003JC002203, 2004.

Hayami Y., Usui S., and Takeoka H.: The stock and long term variation in nitrogen and phosphorus in the Seto Inland Sea, Sea Sky, 80, 75–78, https://doi.org/10.32142/engankaiyo.43.2_129, 2004.

Healy, T. and Harada, K.: Definition and physical characteristics of the world's enclosed coastal seas, Mar. Pollut. Bull., 23, 639–644, https://doi.org/10.1016/0025-326X(91)90749-I, 1991.

Jickells, T. D.: Nutrient Biogeochemistry of the Coastal Zone, Science, 281, 217–222, https://doi.org/10.1126/science.281.5374.217, 1998.

Kawamiya, M.: Mechanism of offshore nutrient supply in the western Arabian Sea, J. Mar. Res., 59, 675–696, https://doi.org/10.1357/002224001762674890, 2001.

Kishi, M. J., Kashiwai, M., Ware, D. M., Megrey, B. A., Eslinger, D. L., Werner, F. E., Noguchi-Aita, M., Azumaya, T., Fujii, M., Hashimoto, S., Huang, D., Iizumi, H., Ishida, Y., Kang, S., Kantakov, G. A., Kim, H., Komatsu, K., Navrotsky, V. V., Smith, S. L., Tadokoro, K., Tsuda, A., Yamamura, O., Yamanaka, Y., Yokouchi, K., Yoshie, N., Zhang, J., Zuenko, Y. I., and Zvalinsky, V. I.: NEMURO—a lower trophic level model for the North Pacific marine ecosystem, Ecol. Model., 202, 12–25, https://doi.org/10.1016/j.ecolmodel.2006.08.021, 2007.

Kobayashi, S. and Fujiwara, T.: Modeling the long-term variability of shelf water intrusion into the Seto Inland Sea, Japan, J. Mar. Syst., 77, 341–349, https://doi.org/10.1016/j.jmarsys.2008.01.012, 2009.

Leppäkoski, E., Shiganova, T., and Alexandrov, B.: European Enclosed and Semi-enclosed Seas, in: Biological Invasions in Marine Ecosystems, vol. 204, edited by: Rilov, G. and Crooks, J. A., Springer Berlin Heidelberg, Berlin, Heidelberg, 529–547, https://doi.org/10.1007/978-3-540-79236-9_30, 2009.

Mackas, D. L. and Harrison, P. J.: Nitrogenous Nutrient Sources and Sinks in the Juan de Fuca Strait/Strait of Georgia/Puget Sound Estuarine System: Assessing the Potential for Eutrophication, Estuar. Coast. Shelf Sci., 44, 1–21, https://doi.org/10.1006/ecss.1996.0110, 1997.

Ménesguen, A., Cugier, P., and Leblond, I.: A new numerical technique for tracking chemical species in a multi-source, coastal ecosystem, applied to nitrogen causing Ulva blooms in the Bay of Brest (France), Limnol. Oceanogr., 51, 591–601, https://doi.org/10.4319/lo.2006.51.1_part_2.0591, 2006.

Morimoto, A., Dong, M., Kameda, M., Shibakawa, T., Hirai, M., Takejiri, K., Guo, X., and Takeoka, H.: Enhanced Cross-Shelf Exchange Between the Pacific Ocean and the Bungo Channel, Japan Related to a Heavy Rain Event, Front. Mar. Sci., 9, 869285, https://doi.org/10.3389/fmars.2022.869285, 2022.

Nakai, S., Soga, Y., Sekito, S., Umehara, A., Okuda, T., Ohno, M., Nishijima, W., and Asaoka, S.: Historical changes in primary production in the Seto Inland Sea, Japan, after implementing regulations to control the pollutant loads, Water Policy, 20, 855–870, https://doi.org/10.2166/wp.2018.093, 2018.

Statham, P. J.: Nutrients in estuaries — An overview and the potential impacts of climate change, Sci. Total Environ., 434, 213–227, https://doi.org/10.1016/j.scitotenv.2011.09.088, 2012.

https://doi.org/10.5194/egusphere-2023-753
Preprint. Discussion started: 2 May 2023

Tada K., Nakajima M., Yamaguchi H., Asahi T., and Ichimi K.: The Nutrient Dynamics and Bottom Sediment in Coastal Water, Bull. Coast. Oceanogr., 55, 113–124, https://doi.org/10.32142/engankaiyo.55.2_113, 2018.

Takashi, T., Fujiwara, T., Sumitomo, T., and Sakamoto, W.: Prediction of slope water intrusion into the Kii channel in summer, J. Oceanogr., 62, 105–113, https://doi.org/10.1007/s10872-006-0037-7, 2006.

Takeoka, H.: Fundamental concepts of exchange and transport time scales in a coastal sea, Cont. Shelf Res., 3, 311–326, https://doi.org/10.1016/0278-4343(84)90014-1, 1984.

Takeoka, H.: Density stratification in the Seto Inland Sea, Umi Sora, 60, 145–152, 1985.

Timmermann, K., Markager, S., and Gustafsson, K. E.: Streams or open sea? Tracing sources and effects of nutrient loadings in a shallow estuary with a 3D hydrodynamic–ecological model, J. Mar. Syst., 82, 111–121, https://doi.org/10.1016/j.jmarsys.2010.04.008, 2010.

Tomita, A., Nakura, Y., and Ishikawa, T.: New direction for environmental water management, Mar. Pollut. Bull., 102, 323–328, https://doi.org/10.1016/j.marpolbul.2015.07.068, 2016.

Tomita, H., Hihara, T., Kako, S., Kubota, M., and Kutsuwada, K.: An introduction to J-OFURO3, a third-generation Japanese ocean flux data set using remote-sensing observations, J. Oceanogr., 75, 171–194, https://doi.org/10.1007/s10872-018-0493-x, 2019.

Townsend, D. W.: Sources and cycling of nitrogen in the Gulf of Maine, J. Mar. Syst., 16, 283–295, https://doi.org/10.1016/S0924-7963(97)00024-9, 1998.

Vermaat, J. E., McQuatters-Gollop, A., Eleveld, M. A., and Gilbert, A. J.: Past, present and future nutrient loads of the North Sea: Causes and consequences, Estuar. Coast. Shelf Sci., 80, 53–59, https://doi.org/10.1016/j.ecss.2008.07.005, 2008.

Wang, X. H.: Tide-Induced Sediment Resuspension and the Bottom Boundary Layer in an Idealized Estuary with a Muddy Bed, J. Phys. Oceanogr., 32, 19, 2002.

Xiu, P. and Chai, F.: Connections between physical, optical and biogeochemical processes in the Pacific Ocean, Prog. Oceanogr., 122, 30–53, https://doi.org/10.1016/j.pocean.2013.11.008, 2014.

Yamamoto, T.: The Seto Inland Sea—eutrophic or oligotrophic?, Mar. Pollut. Bull., 47, 37–42, https://doi.org/10.1016/S0025-326X(02)00416-2, 2003.

Yanagi, T. and Ishii, D.: Open Ocean Originated Phosphorus and Nitrogen in the Seto Inland Sea, Japan, J. Oceanogr., 60, 1001–1005, https://doi.org/10.1007/s10872-005-0008-4, 2004.

Zhang, J., Guo, X., and Zhao, L.: Tracing external sources of nutrients in the East China Sea and evaluating their contributions to primary production, Prog. Oceanogr., 176, 102122, https://doi.org/10.1016/j.pocean.2019.102122, 2019.

Zhu, J., Guo, X., Shi, J., and Gao, H.: Dilution characteristics of riverine input contaminants in the Seto Inland Sea, Mar. Pollut. Bull., 141, 91–103, https://doi.org/10.1016/j.marpolbul.2019.02.029, 2019.